



CHORUS

This is the accepted manuscript made available via CHORUS. The article has been published as:

Distinct critical behaviors from the same state in quantum spin and population dynamics perspectives

C. L. Baldwin, S. Shivam, S. L. Sondhi, and M. Kardar

Phys. Rev. E **103**, 012106 — Published 8 January 2021

DOI: [10.1103/PhysRevE.103.012106](https://doi.org/10.1103/PhysRevE.103.012106)

Distinct Critical Behaviors from the Same State in Quantum Spin and Population Dynamics Perspectives

C. L. Baldwin,^{1,2} S. Shivam,³ S. L. Sondhi,³ and M. Kardar⁴

¹*National Institute of Standards and Technology, Gaithersburg, MD 20899, USA*

²*Joint Quantum Institute, University of Maryland, College Park, MD 20742, USA*

³*Department of Physics, Princeton University, Princeton, New Jersey 08544, USA*

⁴*Department of Physics, Massachusetts Institute of Technology, Cambridge, Massachusetts 02139, USA*

There is a deep connection between the ground states of transverse-field spin systems and the late-time distributions of evolving viral populations – within simple models, both are obtained from the principal eigenvector of the same matrix. However, that vector is the wavefunction amplitude in the quantum spin model, whereas it is the probability itself in the population model. We show that this seemingly minor difference has significant consequences: phase transitions which are discontinuous in the spin system become continuous when viewed through the population perspective, and transitions which are continuous become governed by new critical exponents. We introduce a more general class of models which encompasses both cases, and that can be solved exactly in a mean-field limit. Numerical results are also presented for a number of one-dimensional chains with power-law interactions. We see that well-worn spin models of quantum statistical mechanics can contain unexpected new physics and insights when treated as population-dynamical models and beyond, motivating further studies.

I. INTRODUCTION

A. Viral populations and quantum spins: qualitative comparison

In a somewhat simplified perspective, the evolution of viral populations is governed by two competing processes: mutation of the genetic code upon reproduction, and natural selection due to differences in the corresponding reproduction rates. Mutations destroy the informa-

tion contained in the genetic sequence and lead to a wider variety of sequences in the population (known as a quasi-species cloud), whereas selection promotes those sequences which give the fastest reproduction rates at the expense of slower members. The quasi-species population collapses if the rate of mutations is too large, suggesting a sharp transition – an “error catastrophe” – in the number of mutations per virus [1, 2]. It has motivated the treatment of RNA viruses such as HIV through hypermutation: increasing the average mutation rate in the viral population so as to drastically reduce the proportion of viable members [3–9].

The competition between mutation and selection is analogous to competition between the two terms of a quantum transverse-field Ising model: the transverse field encourages spin flips and leads to a ground state that is superposed from a wider variety of configurations, whereas spin-spin interactions bias the ground state towards specific configurations having lower interaction energy. An error catastrophe simply corresponds to a phase transition in the usual sense of statistical mechanics, i.e., non-analyticity of an observable [10].

B. Viral populations and quantum spins: quantitative comparison

The above analogy has been formulated mathematically and shown to be quite deep [11–15]. Let us briefly summarize the precise relationship.

A particularly simple model for mutation-selection dynamics is to represent genetic sequences by chains of Ising spins: $\sigma \equiv \{\sigma_i\}_{i=1}^N$, where $\sigma_i = -1$ indicates a mutation on site i and $\sigma_i = 1$ indicates no mutation (called “wild-type”). The wild-type state on site i changes to the mutated state at rate Γ_i^+ , and the mutated state reverts to wild-type at rate Γ_i^- . Each sequence σ reproduces at

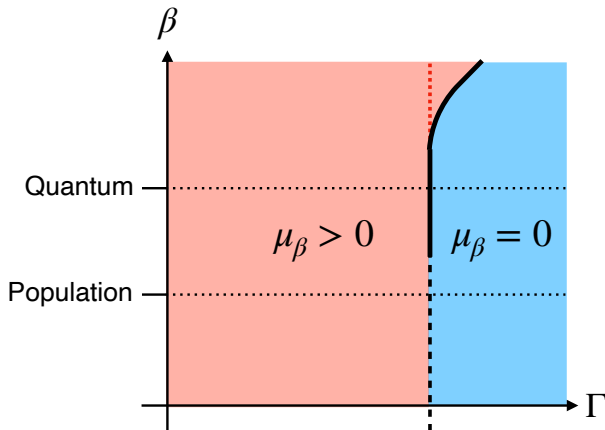


FIG. 1. Sketch of a typical phase diagram in the Γ - β plane, where Γ is the transverse field and β is the power to which the wavefunction amplitude is raised (see the discussion in Sec. IC). Red shading indicates the ordered phase and blue indicates disordered. The black dashed line indicates a continuous transition and solid indicates discontinuous, and the red dashed line is a transition between two ordered phases. The quantum model corresponds to the line $\beta = 2$, and the population dynamics model to $\beta = 1$ (both dotted).

a certain rate $F(\sigma)$, called the fitness function. Natural selection is captured by the fact that different σ have different values of $F(\sigma)$.

A useful measure of the relative strength of mutation versus selection is the surplus μ_1 , defined as the average value throughout the population of $N^{-1} \sum_i \sigma_i$, i.e., the number of wild-type sites minus the number of mutated sites. Clearly smaller Γ_i^\pm and steeper $F(\sigma)$ favor $\mu_1 \approx 1$ (assuming the wild-type state has highest fitness), while larger Γ_i^\pm and shallower $F(\sigma)$ favor $\mu_1 < 1$.

To describe how the population changes over time, we consider the number of members $\mathcal{N}(\sigma, t)$ having each possible sequence σ at time t . Denoting by $L_i \sigma$ the sequence which has spin i flipped relative to σ (e.g., $L_1(1, 1, 1, \dots) = (-1, 1, 1, \dots)$), the time evolution of the population is given by the set of equations

$$\begin{aligned} \frac{d}{dt} \mathcal{N}(\sigma, t) = & F(\sigma) \mathcal{N}(\sigma, t) \\ & + \sum_i (\Gamma_i^{-\sigma_i} \mathcal{N}(L_i \sigma, t) - \Gamma_i^{\sigma_i} \mathcal{N}(\sigma, t)). \end{aligned} \quad (1)$$

The first term is the change due to reproduction, and the second term is that due to mutation. We write Eq. (1) more compactly by denoting $\mathcal{N}(\sigma, t)$ as a vector $|\mathcal{N}(t)\rangle$ in the 2^N -dimensional Hilbert space having basis states $|\sigma\rangle$ (i.e., so that $\langle \sigma | \mathcal{N}(t) \rangle = \mathcal{N}(\sigma, t)$). Evolution according to Eq. (1) is then cast in the matrix form

$$\frac{d}{dt} |\mathcal{N}(t)\rangle = -H |\mathcal{N}(t)\rangle, \quad (2)$$

$$\begin{aligned} H \equiv & -F(\hat{\sigma}^z) + \sum_i \left(\frac{\Gamma_i^+ + \Gamma_i^-}{2} + \frac{\Gamma_i^+ - \Gamma_i^-}{2} \hat{\sigma}_i^z \right) \\ & - \sum_i (\Gamma_i^+ \hat{\sigma}_i^+ + \Gamma_i^- \hat{\sigma}_i^-), \end{aligned} \quad (3)$$

with $\hat{\sigma}$ being the standard Pauli operators.

Equation (3) is quite literally the Hamiltonian of a transverse-field Ising model (albeit non-Hermitian unless $\Gamma_i^+ = \Gamma_i^-$), and Eq. (2) can equally be seen as the imaginary-time Schrodinger equation. In particular, as $t \rightarrow \infty$, the state $|\mathcal{N}(t)\rangle$ approaches the ground state of the Hamiltonian. The steady-state value of the surplus in the population is seen to be a ground state property of the associated Ising Hamiltonian, analogous to the longitudinal magnetization, and any error catastrophe corresponds to a quantum phase transition.

C. Summary of our results

Despite the deep connection between an error catastrophe and a quantum phase transition, the purpose of the present paper is to show that the *nature* of the transition is often qualitatively different when viewed through the surplus rather than the magnetization. There have been observations of this phenomenon previously [14, 16, 17]

(although some specific models have turned out to be misleading [18]), and these observations have been explained in a purely mathematical sense [15, 19]. Yet in our opinion, such explanations, valuable as they are, do not give much physical intuition and risk making the correspondence between the two fields seem less powerful than it is. Our aim in this paper is to study the problem using the techniques and terminology of quantum statistical physics, with the hope of encouraging further investigation of population-dynamical models among the condensed-matter physics community.

One common means of classifying phase transitions is by the non-analyticity of an order parameter, e.g., continuous versus discontinuous. We shall show that the surplus can go to zero continuously even when the magnetization is discontinuous, and can have novel critical exponents at continuous transitions. As will become clear, these differences stem from one detail which was glossed over in the above discussion: the weight $\langle \sigma | \mathcal{N}(t) \rangle$ (once normalized) is the probability of observing configuration σ when sampling randomly from the population, whereas if $|\mathcal{N}(t)\rangle$ were a quantum state it would be the square root of the probability.

Furthermore, we place these results in the context of a larger family of models, taking the probabilities to be the weights $\langle \sigma | \mathcal{N}(t) \rangle$ raised to an arbitrary power β ($\beta = 1$ corresponds to the population dynamics model and $\beta = 2$ corresponds to standard quantum mechanics). This reveals intricate Γ - β phase diagrams, one example of which is sketched in Fig. 1. We show that the nature of the phase transition in Γ can depend on β in a variety of ways, with the overall trends that the transition becomes continuous at lower β and the critical field begins increasing at larger β . The full significance of this non-trivial β -dependence remains to be discovered, but it is already useful in elucidating our results on surplus and magnetization.

Finally, let us briefly mention an alternative perspective on the difference between surplus and magnetization: the distinction between surface and bulk critical phenomena in classical spin systems [16, 20]. We shall postpone a review of the relationship until later in the paper, but the main result (not due to us) is that nonzero surplus corresponds to order at the surface whereas nonzero magnetization corresponds to order in the bulk. This already gives some intuition as to how the two can have different continuity properties: spins at the surface interact with fewer neighbors and have larger fluctuations than in bulk, leading to a suppressed surplus. Our results show that this is sufficient to modify the critical properties quite generically, not only in special cases, and further provide a generalization to arbitrary β (which no longer has the mapping to surface physics).

D. Roadmap

In Sec. II, we present the analytical treatment of symmetric models, i.e., models in which the fitness function depends solely on the total magnetization. Although idealized, they often serve as valuable toy systems among both the statistical physics and population genetics communities [15, 21–24]. We show that the models commonly used to demonstrate discontinuous magnetic phase transitions generically have a continuous surplus. In Sec. III, we then present numerical results demonstrating the same phenomena in non-symmetric models. Although finite-size effects prevent any quantitative conclusions, we do find evidence that the surplus often has distinct critical exponents at continuous phase transitions. Finally, in Sec. IV, we discuss the relationship to critical surface phenomena, and then conclude.

II. EXACT SOLUTION OF SYMMETRIC MODELS

Symmetric Hamiltonians constitute a large family of models for which we can determine the ground state analytically, at least to leading order in large N . By symmetric, we mean any fitness function $F(\sigma)$ which depends only on the total spin- z $M(\sigma) \equiv \sum_i \sigma_i$. An example is

$$F_0(\sigma) = \frac{1}{N} \sum_{i,j} \sigma_i \sigma_j = \frac{1}{N} M(\sigma)^2, \quad (4)$$

which can equivalently be thought of as an Ising model with infinite-range interactions. More generally, we write

$$F(\sigma) = Nf\left(\frac{M(\sigma)}{N}\right), \quad (5)$$

where the factors of N are included simply for convenience in what follows. Furthermore, to make closer contact with the models used in statistical physics, we shall restrict ourselves to Hermitian Hamiltonians ($\Gamma_i^+ = \Gamma_i^-$).

A. Definitions & notation

Taking $|\mathcal{N}\rangle$ to be the ground state of Eq. (3), we denote $\langle \sigma | \mathcal{N} \rangle$ by C_σ . Note that by the Perron-Frobenius theorem, $C_\sigma \geq 0$ for all σ . The symmetry of the Hamiltonian ensures that the eigenstates have definite total angular momentum $\hat{S}^2 \equiv |\sum_i \hat{\sigma}_i|^2$, and we shall focus on the subspace of maximal angular momentum N . In this subspace, C_σ is identical for all configurations having the same $M(\sigma)$. We shall henceforth write C_M , where $M \in \{-N, -N+2, \dots, N\}$.

We will find that C_M is, to leading order, exponentially small in N . In particular,

$$C_M \sim e^{-N\alpha(m)}, \quad (6)$$

for some smooth function α of $m \equiv M/N$.

By definition, the magnetization density of $|\mathcal{N}\rangle$ when viewed as a quantum state is

$$\mu_2 \equiv \frac{1}{N} \frac{\sum_\sigma M(\sigma) C_{M(\sigma)}^2}{\sum_\sigma C_{M(\sigma)}^2}. \quad (7)$$

Correspondingly, the surplus density of $|\mathcal{N}\rangle$ when viewed as a population is

$$\mu_1 \equiv \frac{1}{N} \frac{\sum_\sigma M(\sigma) C_{M(\sigma)}}{\sum_\sigma C_{M(\sigma)}}. \quad (8)$$

Note that we can write

$$\mu_2 = \frac{1}{N} \sum_M M |\Psi(M)|^2, \quad \mu_1 = \frac{1}{N} \sum_M M P(M), \quad (9)$$

where

$$\begin{aligned} |\Psi(M)|^2 &= \frac{\sum_\sigma \delta_{M(\sigma), M} C_{M(\sigma)}^2}{\sum_\sigma C_{M(\sigma)}^2} \propto \left(\frac{N}{\frac{N+M}{2}}\right) C_M^2, \\ P(M) &= \frac{\sum_\sigma \delta_{M(\sigma), M} C_{M(\sigma)}}{\sum_\sigma C_{M(\sigma)}} \propto \left(\frac{N}{\frac{N+M}{2}}\right) C_M, \end{aligned} \quad (10)$$

i.e., $|\Psi(M)|^2$ and $P(M)$ are the probability distributions for the magnetization and surplus respectively.

At large N , the binomial coefficient can be approximated as ($m \equiv M/N$)

$$\binom{N}{\frac{N+M}{2}} \sim e^{Nh(m)}, \quad (11)$$

where

$$h(m) = -\frac{1+m}{2} \log \frac{1+m}{2} - \frac{1-m}{2} \log \frac{1-m}{2}. \quad (12)$$

Using Eq. (6), we have that

$$|\Psi(M)|^2 \propto e^{N(h(m) - 2\alpha(m))}, \quad P(M) \propto e^{N(h(m) - \alpha(m))}. \quad (13)$$

To leading order as $N \rightarrow \infty$,

$$\begin{aligned} \mu_2 &\sim \operatorname{argmax}[h(m) - 2\alpha(m)], \\ \mu_1 &\sim \operatorname{argmax}[h(m) - \alpha(m)]. \end{aligned} \quad (14)$$

where argmax denotes the value of m for which the argument is maximum. Generalizing slightly, we can define an entire family of distributions

$$P_\beta(M) = \frac{\sum_\sigma \delta_{M(\sigma), M} C_{M(\sigma)}^\beta}{\sum_\sigma C_{M(\sigma)}^\beta} \propto e^{Ns_\beta(m)}, \quad (15)$$

where $s_\beta(m) = h(m) - \beta\alpha(m)$, for an arbitrary positive real number β . The generalized magnetization μ_β is defined as the expectation value with respect to $P_\beta(m)$ (hence the notation μ_2 for magnetization and μ_1 for surplus). Although we do not have a physical interpretation

for μ_β at arbitrary β , it will be useful to consider β as a tunable parameter.

In the calculations that follow, it will be easier to work directly with $\Psi(M)$ rather than C_M , thus we give the exponent a name:

$$\frac{1}{N} \log \Psi(M) \equiv \phi(m) = \frac{1}{2} h(m) - \alpha(m). \quad (16)$$

To summarize, in the following section we shall calculate $\phi(m)$, then determine $s_\beta(m)$ via

$$s_\beta(m) = \left(1 - \frac{\beta}{2}\right) h(m) + \beta \phi(m), \quad (17)$$

and finally μ_β via

$$\mu_\beta = \operatorname{argmax}[s_\beta(m)]. \quad (18)$$

B. Large- N analysis

The eigenstates of H in the subspace of maximal angular momentum can be determined analytically using the WKB method, which becomes exact in the $N \rightarrow \infty$ limit. This technique, or equivalent formulations of it, has been applied successfully in both the quantum physics and population genetics fields, and we refer to the literature for further details [13, 15, 23, 25, 26].

Noting that $\langle M|\mathcal{N}\rangle = \Psi(M)$ as defined above (where $|M\rangle$ is the basis state having total spin- z M), we project the eigenvalue equation $E|\mathcal{N}\rangle = H|\mathcal{N}\rangle$ onto $|M\rangle$ to obtain

$$\begin{aligned} E\Psi(M) &= -Nf\left(\frac{M}{N}\right)\Psi(M) \\ &\quad - \frac{\Gamma}{2}\sqrt{(N+M)(N-M+2)}\Psi(M-2) \\ &\quad - \frac{\Gamma}{2}\sqrt{(N-M)(N+M+2)}\Psi(M+2). \end{aligned} \quad (19)$$

We write both $\log \Psi(M)$ and E as series in N :

$$\Psi(M) = e^{N\phi(m) + \phi_1(m) + \frac{1}{N}\phi_2(m) + \dots}, \quad (20)$$

$$E = N\epsilon + \epsilon_1 + \frac{1}{N}\epsilon_2 + \dots, \quad (21)$$

then insert into Eq. (19) and equate like powers of N (while expanding terms like $\phi(m \pm \frac{2}{N})$ in Taylor series). For our purposes, only the $O(N)$ equation will be needed. It is

$$\epsilon = -f(m) - \Gamma\sqrt{1-m^2} \cosh\left(2\frac{d\phi}{dm}\right). \quad (22)$$

Solving for $d\phi/dm$, we have

$$\begin{aligned} \frac{d\phi}{dm} &= \frac{1}{2} \log\left(\kappa(m) \pm \sqrt{\kappa(m)^2 - 1}\right), \\ \kappa(m) &\equiv \frac{-\epsilon - f(m)}{\Gamma\sqrt{1-m^2}}. \end{aligned} \quad (23)$$

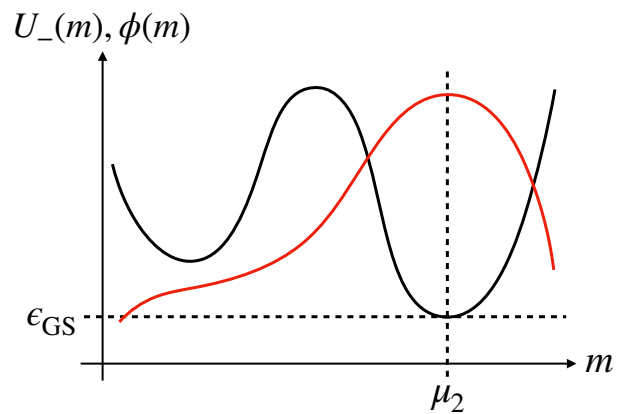


FIG. 2. Sketch of an example potential $U_-(m)$ (solid black line), the ground state energy density ϵ_{GS} and average magnetization μ_2 , and the resulting wavefunction exponent $\phi(m)$ (red line).

As discussed in Appendix A, the correct sign to use in Eq. (23) is the plus sign near $m = -1$ and the minus sign near $m = 1$, needed so that Eq. (23) agrees with the Schrodinger equation at the endpoints (for which a separate expansion is needed). This then requires that $|\kappa(m)|$ cross 1 at some intermediate value of m , so that $d\phi/dm$ is non-analytic there [27]. The requirement that $|\kappa(m)| \leq 1$ for at least one point m translates to a restriction on the allowed values of ϵ : there must be a point m at which

$$\begin{aligned} U_-(m) &\leq \epsilon \leq U_+(m), \\ U_\pm(m) &\equiv -f(m) \pm \Gamma\sqrt{1-m^2}. \end{aligned} \quad (24)$$

The ground state energy is the lowest allowed value:

$$\epsilon_{\text{GS}} = \min_m [U_-(m)]. \quad (25)$$

These equations are best understood graphically, such as in Fig. 2.

Equation (24) further has a nice physical interpretation: Consider a classical spin \hat{s} , by which we mean a unit vector in \mathbb{R}^3 , with an energy function $H_{\text{cl}}(\hat{s})$ analogous to the original Hamiltonian:

$$H_{\text{cl}}(\hat{s}) = -f(s_z) - \Gamma s_x, \quad (26)$$

where s_x and s_z are the projections along the x and z axes. If s_z is fixed to be m , then s_x can take values between $-\sqrt{1-m^2}$ and $\sqrt{1-m^2}$. $U_+(m)$ and $U_-(m)$ are precisely the maximum and minimum corresponding energies, and the lowest possible energy is found by minimizing $U_-(m)$, i.e., Eq. (25).

The magnetization density of the ground state is correspondingly

$$\mu_2 = \operatorname{argmin}_m [U_-(m)]. \quad (27)$$

This follows from having $d\phi/dm > 0$ for m less than the argmin and $d\phi/dm < 0$ for m greater than the argmin:

$$\frac{d\phi}{dm} = \begin{cases} \frac{1}{2} \log \left(\kappa(m) + \sqrt{\kappa(m)^2 - 1} \right), & m \leq \text{argmin}[U_-] \\ \frac{1}{2} \log \left(\kappa(m) - \sqrt{\kappa(m)^2 - 1} \right), & m \geq \text{argmin}[U_-] \end{cases} \quad (28)$$

Thus $\phi(m)$ is maximized at the argmin. Since μ_2 is the sum over M of $M|\Psi(M)|^2$ and $\Psi(M)$ scales exponentially with N , the sum is dominated by where the exponent is maximal, giving Eq. (27). The situation is sketched in Fig. 2.

With this analysis in hand, we now calculate $\phi(m)$ and $s_\beta(m)$ for a variety of symmetric Hamiltonians. The locations of the maxima of $s_\beta(m)$ then give the values of μ_β shown in what follows (see Eqs. (17) and (18)).

C. Results

For concreteness, we have focused on systems which exhibit a transition from an ordered phase having magnetization $\mu_2 > 0$ to a disordered phase having $\mu_2 = 0$ as Γ is increased. A sufficient condition is that the fitness function $f(m)$ increase monotonically with m and grow no faster than $O(m^2)$ near $m = 0$. For example, $f(m) = m^2 \text{sgn}[m]$ and $f(m) = m^3$ both exhibit such a transition, as shown in Fig. 3. Note that the former undergoes a continuous transition (in that μ decreases to 0 continuously) whereas the latter is discontinuous.

The corresponding μ_β for these examples are shown in Fig. 4. Considering the upper panel, we see that as $\Gamma \rightarrow \Gamma_c$ from below, the magnetization μ_2 vanishes as $\sqrt{\Gamma_c - \Gamma}$ but the surplus μ_1 vanishes more rapidly as $\Gamma_c - \Gamma$ (the precise scaling can easily be verified analytically). In the language of critical exponents, the magnetization has exponent 1/2 whereas the surplus has exponent 1.

The contrast is even more stark in the lower panel: whereas μ_2 remains finite as $\Gamma \rightarrow \Gamma_c$, μ_1 vanishes. This behavior is quite generic. Fig. 5 presents the magnetization and surplus for a wide variety of fitness functions, all chosen so that the transition in magnetization is discontinuous. In all cases, the transition in surplus is nonetheless continuous.

Furthermore, one can prove that the surplus transition is continuous for *any* model which meets our two criteria stated above (namely that $f(m)$ increases monotonically and grows no faster than $O(m^2)$ near $m = 0$). The proof is given in Appendix B.

Our goal is now to understand this phenomenon in more physical terms. In doing so, it will be convenient to consider the parameter β as an arbitrary positive real number. For reference, recall the expressions

$$\begin{aligned} \mu_2 &= \text{argmin}_m [U_-(m)], & \epsilon_{\text{GS}} &= U_-(\mu_2), \\ \kappa(m) &\equiv 1 + \frac{U_-(m) - \epsilon_{\text{GS}}}{\Gamma \sqrt{1 - m^2}}, \end{aligned} \quad (29)$$

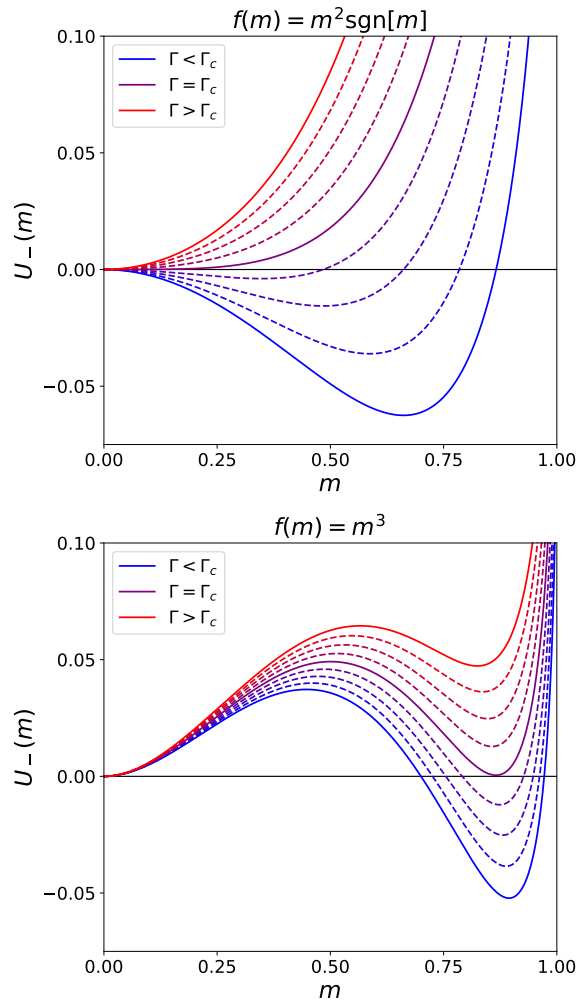


FIG. 3. Two examples of the potential $U_-(m)$ as a function of m , for various Γ (increasing from blue curves to red). The fitness functions $f(m)$ are indicated, and the potential is given by Eq. (24). For this figure, constants have been added to $U_-(m)$ so that $U_-(0) = 0$. (Top) A potential which gives a continuous transition. Solid curves are $\Gamma = 1.5, 2.0, 2.5$ (blue to red). (Bottom) A potential which gives a discontinuous transition. Solid curves are $\Gamma = 1.2, 1.3, 1.4$.

from which the exponent of the ground state wavefunction is, for $m \leq \mu_2$ (see Eq. (28)),

$$\phi(m) = -\frac{1}{2} \int_m^{\mu_2} dm \log \left(\kappa(m) + \sqrt{\kappa(m)^2 - 1} \right), \quad (30)$$

and the generalized magnetization μ_β is given by

$$\begin{aligned} \mu_\beta &= \text{argmax}_m [s_\beta(m)], \\ s_\beta(m) &= \left(1 - \frac{\beta}{2} \right) h(m) + \beta \phi(m), \end{aligned} \quad (31)$$

where $h(m)$, the “binomial entropy,” is given by Eq. (12). We are setting $\phi(\mu_2) = 0$ for convenience.

Note that the numerator of $\kappa(m) - 1$ is the height of the potential barrier, $U_-(m) - \epsilon_{\text{GS}}$. Furthermore, $d\phi/dm$ in-

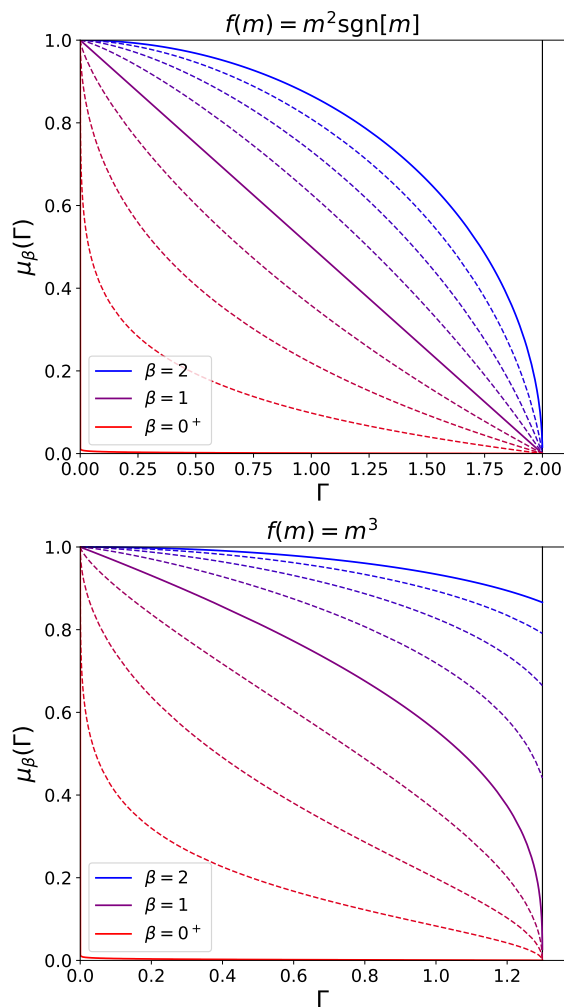


FIG. 4. Generalized magnetization μ_β as a function of Γ , for various β (decreasing from blue to red) and the same fitness functions as in Fig. 3. The vertical black lines indicate the values of Γ_c (μ_β is identically 0 for $\Gamma > \Gamma_c$).

creases monotonically with $\kappa(m)$. Thus the wavefunction behaves roughly as one would find in the WKB treatment of 1D tunneling problems: the slope is zero only at points where the barrier vanishes, and the wavefunction falls off faster in regions where the barrier is larger (albeit with the factor of $\Gamma\sqrt{1-m^2}$ included). Figure 6 gives an example. Note that the qualitative features of $\phi(m)$ can be predicted simply from the shape of $U_-(m)$.

First consider $\beta < 2$. A number of results follow immediately from the above discussion:

- The surplus is less than the magnetization — this follows from the fact that $ds_\beta/dm|_{m=\mu_2} < 0$ for $\beta < 2$.
- The surplus is non-negative — this follows from $ds_\beta/dm > 0$ for $m < 0$.
- The surplus is positive for all $\Gamma < \Gamma_c$ — this follows from $d\phi/dm|_{m=0} > 0$ (since $U_-(0) > \epsilon_{GS}$) and thus

$$ds_\beta/dm|_{m=0} > 0.$$

- The surplus is strictly zero for all $\Gamma > \Gamma_c$ — both $d\phi/dm$ and $(1-\beta/2)h(m)$ are maximized at $m = 0$ when $\Gamma > \Gamma_c$.

Note that all these features are borne out in Fig. 4.

The maximization of $s_\beta(m)$ can be thought of as a competition between two terms. The binomial contribution $h(m)$ is an entropic term, in that it is maximal at $m = 0$ and strictly concave everywhere. The wavefunction $\phi(m)$ is an energetic term (although not literally an energy), since it is maximal at $m = \mu_2$. β then plays a role analogous to the inverse temperature in a thermal ensemble: in one limit ($\beta = 0$), the entropic term dominates; in another limit ($\beta = 2$), the energetic term dominates; and for β in between, the maximum is at an intermediate value of m .

These considerations together explain why μ_β lowers continuously to 0 as $\Gamma \rightarrow \Gamma_c$, at least for small β . The wavefunction $\phi(m)$ is a small perturbation to $h(m)$ when β is small, and in particular $s_\beta(m)$ will be strictly concave for β less than a certain non-zero value. The strict concavity ensures that μ_β varies continuously with Γ , and since we know that $\mu_\beta = 0$ at $\Gamma = \Gamma_c$, it follows that $\mu_\beta \rightarrow 0$ as $\Gamma \rightarrow \Gamma_c$.

Of course, this argument does not prove that μ_1 , the quantity which we are most interested in, must approach 0. That proof is supplied in Appendix B, where we show that $s_1(m)$ cannot be maximized at $m \sim O(1)$ as $\Gamma \rightarrow \Gamma_c$. In this sense, $\beta = 1$ is sufficiently “small” for the above argument to hold. The critical value of β separating continuous from discontinuous μ_β can generically be anywhere between 1 and 2, depending on the fitness function.

It is interesting to note that in models with flat fitness functions, such as the single-peak landscape often studied in the literature [16, 18], these conclusions no longer hold. In particular, one can verify that the surplus of the single-peak landscape ($f(\sigma) = \delta_{m,1}$) is discontinuous: the surplus jumps from 1 to 0 at $\Gamma = 1$. The situation also becomes more complex if one allows for alternate configuration spaces, such as the truncated configuration space considered in Ref. [17]. In that model, the authors demonstrated that the surplus and magnetization transitions can occur at different values of Γ .

Finally, let us briefly consider $\beta > 2$. The entropy term $(1-\beta/2)h(m)$ is now convex, and is minimized at $m = 0$ rather than maximized. Thus $\mu_\beta > \mu_2$. As a result, μ_β need not be zero for all $\Gamma > \Gamma_c$, although it is certainly non-analytic at Γ_c . We generically find the behaviors indicated in Fig. 7: if the transition in μ_2 is continuous, then the transitions in all μ_β will be as well, but at fields increasing with β . One can confirm that the critical exponents are the same as for the magnetization, i.e., those of standard mean-field theory. For discontinuous transitions, the critical field remains at the original Γ_c for β less than a certain model-dependent value, past which it increases with β . In its place at the original Γ_c remains

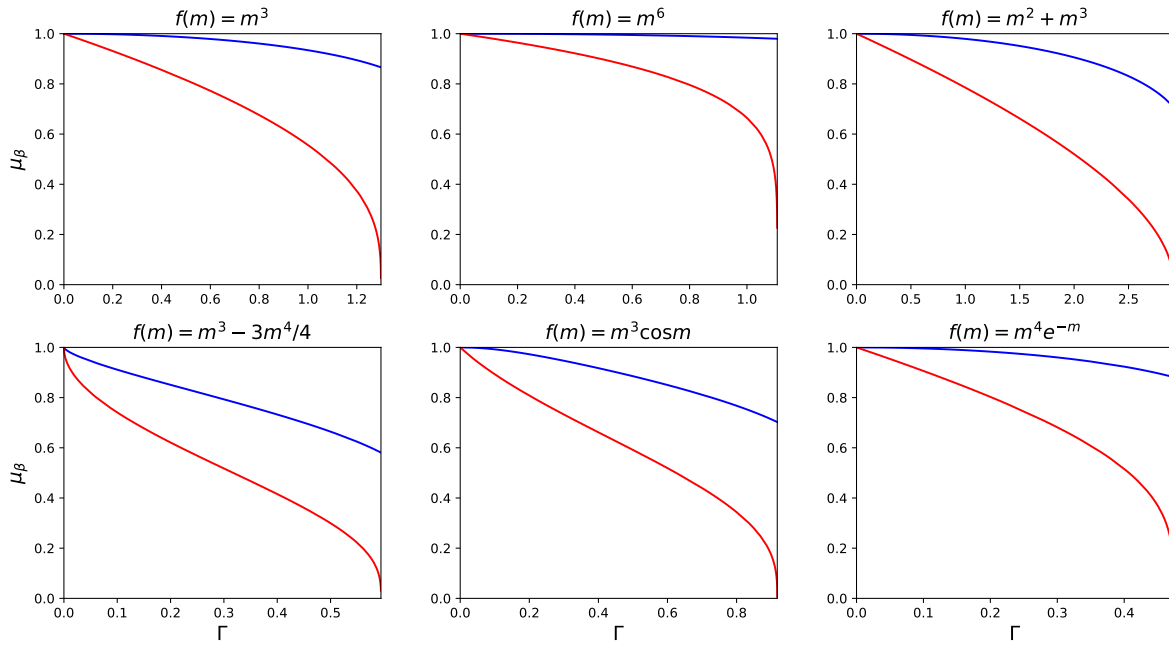


FIG. 5. Comparison of magnetization (blue, $\beta = 2$) against surplus (red, $\beta = 1$) for many different fitness functions. In all plots, the right-most value of Γ is the transition point Γ_c .

an ordered-to-ordered transition, which is always continuous: since $d\phi/dm$ is continuous at Γ_c for all $m > \mu_2$ (see Eq. (28) and note that $m > \text{argmin}[U_-]$ both above and below Γ_c), so is the solution to the equation $ds_\beta/dm = 0$. The resulting phase diagram is sketched in Fig. 1.

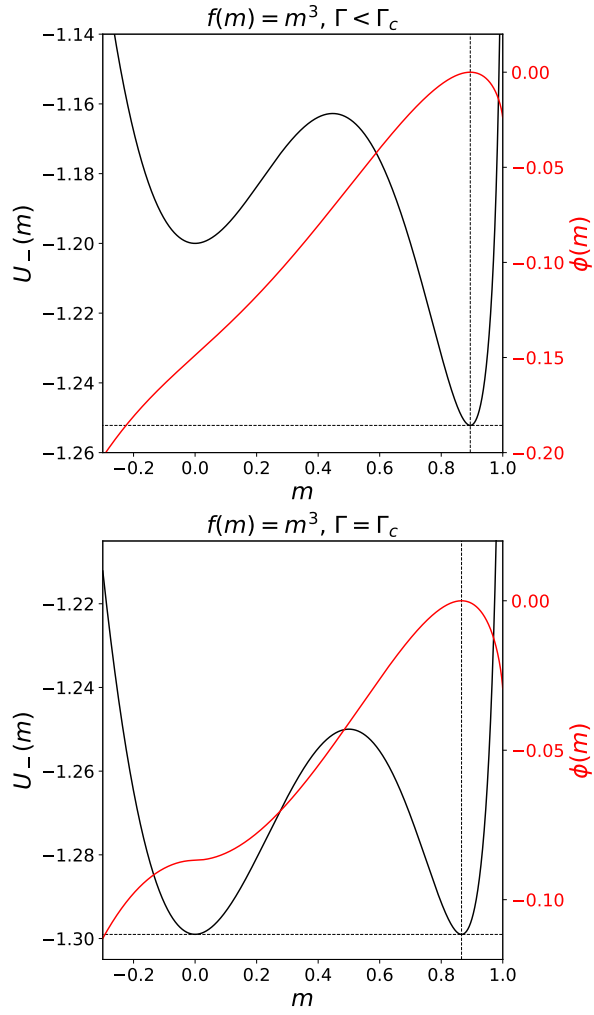


FIG. 6. Wavefunction $\phi(m)$ for the $f(m) = m^3$ fitness function, both for a value of Γ less than Γ_c (top) and $\Gamma = \Gamma_c$ (bottom). Wavefunctions are in red, while the corresponding potentials $U_-(m)$ are shown in black, with ϵ_{GS} and μ indicated by dashed lines. The precise values of Γ are 1.2 (top) and 1.299 (bottom).

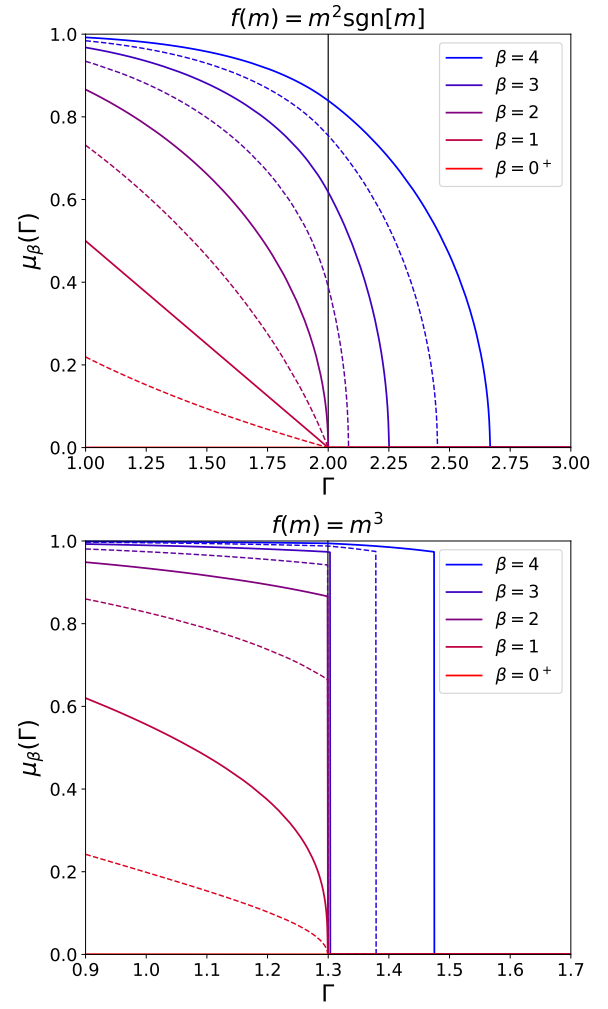


FIG. 7. Generalized magnetization μ_β as a function of Γ , for various β both greater than and less than 2 (decreasing from blue to red). Fitness functions are indicated above each plot. The vertical black lines indicate Γ_c for the quantum transition ($\beta = 2$).

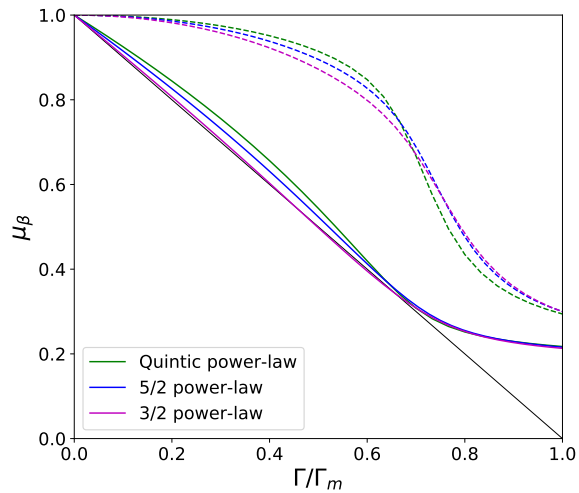


FIG. 8. Surplus (solid lines) and magnetization (dashed lines) as functions of transverse field, for the Ising models in Eqs. (32), (33), and (34). System size is $N = 22$. For each model, Γ_m is the field at which $\mu_2 = 0.3$, chosen simply to normalize the x axis (since the three models have significantly different Γ_c). The solid black line is merely a straight line drawn for comparison.

III. NUMERICAL RESULTS FOR SHORT-RANGE MODELS

To reiterate, our analysis of symmetric models identified two important differences between the magnetization and surplus at the critical point: in situations where the magnetization approaches 0 continuously, the surplus is characterized by a different critical exponent ($\mu_1 \sim \Gamma_c - \Gamma$ vs $\mu_2 \sim \sqrt{\Gamma_c - \Gamma}$); and in situations where the magnetization is discontinuous, the surplus is nonetheless continuous. The rough intuition is that the surplus is more influenced by the entropic effect of there being more configurations having small total spin- z than large. Yet the analysis used to derive these results relied heavily on the model being symmetric, thus we now investigate whether the conclusions extend to more general systems.

We study a series of one-dimensional transverse-field Ising models through exact diagonalization of the Hamiltonian. Unfortunately, the accessible system sizes are too small to draw any quantitative conclusions. One could perform a more systematic study using quantum Monte Carlo – note that the models considered here do not have sign problems – together with a finite-size scaling analysis, but we leave that for future work. The purpose of this section is merely to provide preliminary evidence suggesting that the surplus and magnetization exhibit different critical properties even in non-symmetric models.

One such Hamiltonian, the nearest-neighbor ferromagnetic chain, can be solved analytically as was done in Ref. [11]. The authors showed that the surplus undergoes a non-analyticity at the same Γ_c as the magnetization, but with an exponent of 1/2 rather than the well-known 1/8 of the magnetization (see also Ref. [28]).

Here we consider the following fitness functions, all of which are for an N -site chain:

$$F_5(\hat{\sigma}^z) = \sum_{i < j} \frac{1}{|i - j|^5} \hat{\sigma}_i^z \hat{\sigma}_j^z, \quad (32)$$

$$F_{5/2}(\hat{\sigma}^z) = \sum_{i < j} \frac{1}{|i - j|^{5/2}} \hat{\sigma}_i^z \hat{\sigma}_j^z, \quad (33)$$

$$F_{3/2}(\hat{\sigma}^z) = \sum_{i < j} \frac{1}{|i - j|^{3/2}} \hat{\sigma}_i^z \hat{\sigma}_j^z, \quad (34)$$

$$F_{\text{Four}}(\hat{\sigma}^z) = \sum_i \hat{\sigma}_i^z \hat{\sigma}_{i+1}^z - \sum_i \hat{\sigma}_i^z \hat{\sigma}_{i+1}^z \hat{\sigma}_{i+2}^z \hat{\sigma}_{i+3}^z. \quad (35)$$

These models do not have analytic solutions, but it is known that the quintic power-law model F_5 has the same magnetization exponents as the nearest-neighbor chain, the 3/2 power-law model $F_{3/2}$ has those of mean-field theory, and the 5/2 model $F_{5/2}$ has intermediate exponents [29, 30]. In general, longer-range interactions have a larger exponent governing the magnetization. The results shown in Fig. 8 are qualitatively consistent with

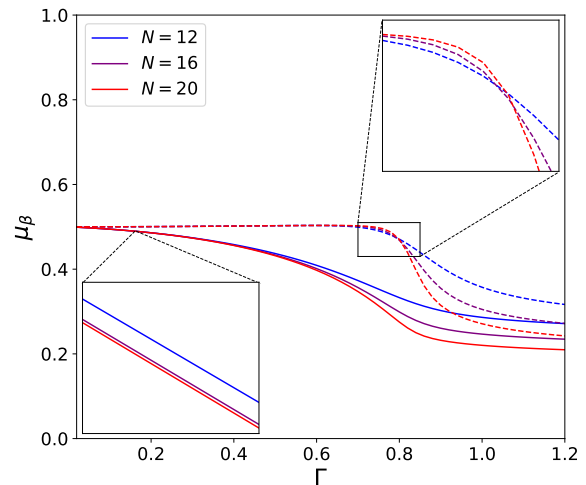


FIG. 9. Surplus (solid lines) and magnetization (dashed lines) for the Ising model with four-spin interactions, Eq. (35). Insets show magnified portions of the plot, demonstrating that the magnetization curves cross each other whereas the surplus curves decrease monotonically with N even at small Γ .

this trend – the curvature of the curves is smaller for the longer-range models – and we see that the same trend holds for the surplus. Again, these observations are hardly quantitative and the differences are quite modest. One feature which is reasonably clear, however, is that the surplus seems to have a larger exponent than the magnetization in all cases shown.

As for Eq. (35), the model with antiferromagnetic four-spin interactions, it has been shown to exhibit a discontinuity in magnetization as one increases Γ [31]. Figure 9 shows the surplus and magnetization for F_{Four} . Even though the small system sizes again prohibit quantitative statements, we see that the magnetization curves are consistent with a discontinuous transition: the fall-off near the transition region becomes sharper as system size increases. The surplus curves do not show any such behavior, and instead are more consistent with a continuous transition. It thus appears that even in non-symmetric models, the surplus and magnetization transitions can have different orders.

We have not been able to reach any conclusions regarding $\beta > 2$ – finite size effects are too severe – but we expect the behavior seen in symmetric models to apply here as well, namely that μ_β remains non-zero at Γ_c (albeit non-analytically) for sufficiently large β . The intuition is again that μ_β is shifted relative to μ_2 by an entropic effect, but with the entropic correction now acting to keep $\mu_\beta \neq 0$ at Γ_c . There are many interesting questions, e.g., the nature of the non-analyticity at Γ_c and whether μ_β drops to zero at larger fields, and a more systematic study is clearly warranted.

IV. DISCUSSION & CONCLUSION

Many quantum spin Hamiltonians can serve as generators for the evolution of populations under joint mutation and selection, and quantum phase transitions are then associated with error catastrophes. We have shown here that despite the correspondence between the spin magnetization and the population surplus, the continuity properties of the two can be different. Transitions in which the magnetization is discontinuous often have a surplus which remains continuous, while continuous transitions come with novel critical exponents for the surplus.

There is a third perspective through which to view these results: the different critical properties of free surfaces as compared to bulk in classical Ising models. It

is well-known that d -dimensional quantum Ising systems can be mapped to $(d+1)$ -dimensional classical systems, and it is also well-documented that systems with open boundary conditions can have different critical exponents or even orders of transitions at the free surfaces.

To see explicitly that the surplus in mutation-selection models corresponds to a surface magnetization, note that the time evolution of the population (say starting from a specific sequence $\sigma^{(0)}$) can be written compactly as

$$\mathcal{N}(\sigma, t) = \langle \sigma | \mathcal{N}(t) \rangle = \langle \sigma | e^{-Ht} | \sigma^{(0)} \rangle, \quad (36)$$

which can then be expressed through standard means as the partition function of a classical system. For example, in the transverse-field models considered here,

$$\begin{aligned} \mathcal{N}(\sigma, t) &= \sum_{\sigma^{(1)} \dots \sigma^{(M-1)}} \langle \sigma | e^{-H \frac{t}{M}} | \sigma^{(M-1)} \rangle \langle \sigma^{(M-1)} | \dots | \sigma^{(1)} \rangle \langle \sigma^{(1)} | e^{-H \frac{t}{M}} | \sigma^{(0)} \rangle \\ &\sim \sum_{\sigma^{(1)} \dots \sigma^{(M-1)}} \exp \left[\sum_{m=0}^{M-1} \left(\frac{t}{M} F(\sigma^{(m)}) + V(\sigma^{(m+1)}, \sigma^{(m)}) \right) \right], \end{aligned} \quad (37)$$

where $V(\sigma, \sigma') \equiv \frac{1}{2} \log \coth \frac{\Gamma t}{M} \sum_i \sigma_i \sigma'_i$ plus a constant (with $M \rightarrow \infty$ implied). We see that the transverse field corresponds to a ferromagnetic interaction between $\sigma^{(m)}$ and $\sigma^{(m+1)}$, regardless of the form of the fitness function.

Note that in Eq. (37), $\sigma^{(M)}$ is fixed at σ . It is also a “surface” layer of spins, in that there is no $\sigma^{(M+1)}$ to interact with. Finally, to compute the average over the population of any quantity $g(\sigma)$, we evaluate

$$\sum_{\sigma} g(\sigma) \frac{\mathcal{N}(\sigma, t)}{\sum_{\sigma'} \mathcal{N}(\sigma', t)} \propto \sum_{\sigma^{(1)} \dots \sigma^{(M)}} g(\sigma^{(M)}) \exp \left[\dots \right], \quad (38)$$

where \dots denotes the exponent in Eq. (37). For the surplus in particular, we see that it is precisely the average magnetization of the surface layer in the classical Ising model.

This relationship was first discussed in Ref. [20], and indeed, many of the previous works comparing surplus to magnetization have been in the language of surface versus bulk magnetization [16, 32]. In particular, the continuity of magnetization at the surface despite discontinuity in the bulk has been understood as an example of “wetting”. The existence of novel surface exponents has also been well-studied in that context [33–35].

Of course, these considerations alone do not prove that the surplus must behave differently than magnetization at the transition point. Rather, they simply raise the possibility. The results we have presented here show that it is indeed a generic phenomenon which occurs in practice.

It is clear that the techniques and ideas of quantum statistical physics can fruitfully be applied to problems in population dynamics. At the same time, as the above

results demonstrate, the population-dynamical analogues of quantum spin systems exhibit novel behaviors which are not simple corollaries to the quantum physics. The former can also be considered in situations where the latter cannot, such as non-Hermitian models [36]. Further investigation of quantum systems as population-dynamical models and vice-versa will undoubtedly uncover additional surprises and insights for both fields.

Finally, there is the question of whether the generalized magnetization μ_{β} has physical significance for *arbitrary* β . This larger family of observables is useful for understanding the distinction between surplus and magnetization, as can be seen in Fig. 1, and it would be valuable to know what other information is contained in the Γ - β phase diagram. There are contexts in which one considers a probability distribution raised to arbitrary powers. For example, Ref. [37] has recently shown that, for certain classes of quantum Hamiltonians, exponentiating the reduced density matrix obtained from an eigenstate at some energy density allows one to probe properties of the system at different energy densities. Similarly, Ref. [38] has demonstrated that raising the reduced density matrix to a large power, as had been done in studies of topological order [39, 40], can introduce spurious phase transitions not seen in the original system. Two other situations which come to mind are calculation of Renyi entropies (both classical [41] and quantum [42]) and multifractality [43–45], and we certainly expect that these are not the only examples. The implications of our results in these areas is a topic for further study.

V. ACKNOWLEDGEMENTS

The authors would like to thank the Galileo Galilei Institute for Theoretical Physics and the organizers of the workshop “Breakdown of Ergodicity in Isolated Quantum Systems: From Glassiness to Localization”, where this work was begun. This research was performed while

C.L.B. held a National Institute of Standards and Technology (NIST) National Research Council (NRC) Research Postdoctoral Associateship Award. MK is supported by NSF through grant No. DMR-1708280 and SLS by the United States Department of Energy via grant No. DE-SC0016244. Additional support was provided by the Gordon and Betty Moore Foundation through Grant GBMF8685 towards the Princeton theory program.

-
- [1] M. Eigen, “Selforganization of matter and the evolution of biological macromolecules,” *Naturwissenschaften*, vol. 58, pp. 465–523, Oct 1971.
- [2] C. O. Wilke, “Quasispecies theory in the context of population genetics,” *BMC Evolutionary Biology*, vol. 5, no. 1, p. 44, 2005.
- [3] S. Crotty, C. E. Cameron, and R. Andino, “Rna virus error catastrophe: Direct molecular test by using ribavirin,” *Proceedings of the National Academy of Sciences*, vol. 98, p. 6895, 06 2001.
- [4] H. Zhang, B. Yang, R. J. Pomerantz, C. Zhang, S. C. Arunachalam, and L. Gao, “The cytidine deaminase *cem15* induces hypermutation in newly synthesized hiv-1 dna,” *Nature*, vol. 424, no. 6944, pp. 94–98, 2003.
- [5] J. P. Anderson, R. Daifuku, and L. A. Loeb, “Viral error catastrophe by mutagenic nucleosides,” *Annual Review of Microbiology*, vol. 58, pp. 183–205, 2020/08/18 2004.
- [6] A. Grande-Pérez, E. Lázaro, P. Lowenstein, E. Domingo, and S. C. Manrubia, “Suppression of viral infectivity through lethal defection,” *Proceedings of the National Academy of Sciences of the United States of America*, vol. 102, p. 4448, 03 2005.
- [7] G. R. Hart and A. L. Ferguson, “Error catastrophe and phase transition in the empirical fitness landscape of hiv,” *Phys. Rev. E*, vol. 91, p. 032705, Mar 2015.
- [8] V. Gupta and N. M. Dixit, “Scaling law characterizing the dynamics of the transition of HIV-1 to error catastrophe,” *Physical Biology*, vol. 12, p. 054001, sep 2015.
- [9] S. Shivam, C. L. Baldwin, J. Barton, M. Kardar, and S. L. Sondhi, “Studying viral populations with tools from quantum spin chains,” *arXiv:2003.10668*, 2020.
- [10] Many works use a slightly different definition of error catastrophe, namely when the fraction of wild-type states in the population becomes zero. We use the definition involving average surplus because it is more natural from a statistical-physics perspective. See as well Ref. [18].
- [11] E. Baake, M. Baake, and H. Wagner, “Ising quantum chain is equivalent to a model of biological evolution,” *Phys. Rev. Lett.*, vol. 78, pp. 559–562, Jan 1997.
- [12] H. Wagner, E. Baake, and T. Gerisch, “Ising quantum chain and sequence evolution,” *Journal of Statistical Physics*, vol. 92, pp. 1017–1052, Sep 1998.
- [13] E. Baake and H. Wagner, “Mutation–selection models solved exactly with methods of statistical mechanics,” *Genetical Research*, vol. 78, no. 1, pp. 93–117, 2001.
- [14] J. Hermisson, H. Wagner, and M. Baake, “Four-state quantum chain as a model of sequence evolution,” *Journal of Statistical Physics*, vol. 102, no. 1, pp. 315–343, 2001.
- [15] J. Hermisson, O. Redner, H. Wagner, and E. Baake, “Mutation–selection balance: Ancestry, load, and maximum principle,” *Theoretical Population Biology*, vol. 62, no. 1, pp. 9–46, 2002.
- [16] P. Tarazona, “Error thresholds for molecular quasispecies as phase transitions: From simple landscapes to spin-glass models,” *Phys. Rev. A*, vol. 45, pp. 6038–6050, Apr 1992.
- [17] D. B. Saakian, C. K. Biebricher, and C.-K. Hu, “Phase diagram for the eigen quasispecies theory with a truncated fitness landscape,” *Phys. Rev. E*, vol. 79, p. 041905, Apr 2009.
- [18] S. Franz and L. Peliti, “Error threshold in simple landscapes,” *Journal of Physics A: Mathematical and General*, vol. 30, pp. 4481–4487, jul 1997.
- [19] E. Baake, M. Baake, and H. Wagner, “Quantum mechanics versus classical probability in biological evolution,” *Phys. Rev. E*, vol. 57, pp. 1191–1192, Jan 1998.
- [20] I. Leuthäusser, “Statistical mechanics of eigen’s evolution model,” *Journal of Statistical Physics*, vol. 48, no. 1, pp. 343–360, 1987.
- [21] L. Peliti, “Quasispecies evolution in general mean-field landscapes,” *Europhysics Letters (EPL)*, vol. 57, pp. 745–751, mar 2002.
- [22] D. B. Saakian, C.-K. Hu, and H. Khachatryan, “Solvable biological evolution models with general fitness functions and multiple mutations in parallel mutation–selection scheme,” *Phys. Rev. E*, vol. 70, p. 041908, Oct 2004.
- [23] V. Bapst and G. Semerjian, “On quantum mean-field models and their quantum annealing,” *Journal of Statistical Mechanics: Theory and Experiment*, vol. 2012, no. 06, p. P06007, 2012.
- [24] B. Zhao, M. C. Kerridge, and D. A. Huse, “Three species of schrödinger cat states in an infinite-range spin model,” *Phys. Rev. E*, vol. 90, p. 022104, Aug 2014.
- [25] A. Garg, “Application of the discrete wenzel–kramers–brillouin method to spin tunneling,” *Journal of Mathematical Physics*, vol. 39, no. 10, pp. 5166–5179, 1998.
- [26] D. B. Saakian, “A new method for the solution of models of biological evolution: Derivation of exact steady-state distributions,” *Journal of Statistical Physics*, vol. 128, no. 3, pp. 781–798, 2007.
- [27] This is analogous to the situation in single-particle bound state problems, where states must have energies greater than the minimum of the potential in order to be normalizable.
- [28] C. Kaiser and I. Peschel, “Surface and corner magnetizations in the two-dimensional ising model,” *Journal of Statistical Physics*, vol. 54, no. 3, pp. 567–579, 1989.
- [29] A. Dutta and J. K. Bhattacharjee, “Phase transitions in the quantum ising and rotor models with a long-range interaction,” *Phys. Rev. B*, vol. 64, p. 184106, Oct 2001.

- [30] S. Fey and K. P. Schmidt, “Critical behavior of quantum magnets with long-range interactions in the thermodynamic limit,” *Phys. Rev. B*, vol. 94, p. 075156, Aug 2016.
- [31] O. F. de Alcantara Bonfim and J. Florencio, “Quantum phase transitions in the transverse one-dimensional ising model with four-spin interactions,” *Phys. Rev. B*, vol. 74, p. 134413, Oct 2006.
- [32] S. Franz, L. Peliti, and M. Sellitto, “An evolutionary version of the random energy model,” *Journal of Physics A: Mathematical and General*, vol. 26, pp. L1195–L1199, dec 1993.
- [33] K. Binder and P. C. Hohenberg, “Phase transitions and static spin correlations in ising models with free surfaces,” *Phys. Rev. B*, vol. 6, pp. 3461–3487, Nov 1972.
- [34] R. Lipowsky, “Surfaceinduced order and disorder: Critical phenomena at firstorder phase transitions (invited),” *Journal of Applied Physics*, vol. 55, pp. 2485–2490, 2020/01/06 1984.
- [35] K. Binder and D. P. Landau, “Critical phenomena at surfaces,” *Physica A: Statistical Mechanics and its Applications*, vol. 163, no. 1, pp. 17–30, 1990.
- [36] D. B. Saakian and C.-K. Hu, “Exact solution of the eigen model with general fitness functions and degradation rates,” *Proceedings of the National Academy of Sciences of the United States of America*, vol. 103, p. 4935, 03 2006.
- [37] J. R. Garrison and T. Grover, “Does a single eigenstate encode the full hamiltonian?,” *Phys. Rev. X*, vol. 8, p. 021026, Apr 2018.
- [38] A. Chandran, V. Khemani, and S. L. Sondhi, “How universal is the entanglement spectrum?,” *Phys. Rev. Lett.*, vol. 113, p. 060501, Aug 2014.
- [39] H. Li and F. D. M. Haldane, “Entanglement spectrum as a generalization of entanglement entropy: Identification of topological order in non-abelian fractional quantum hall effect states,” *Phys. Rev. Lett.*, vol. 101, p. 010504, Jul 2008.
- [40] N. Regnault and B. A. Bernevig, “Fractional chern insulator,” *Phys. Rev. X*, vol. 1, p. 021014, Dec 2011.
- [41] A. Renyi, “On measures of entropy and information,” pp. 547–561, 1961.
- [42] M. Müller-Lennert, F. Dupuis, O. Szehr, S. Fehr, and M. Tomamichel, “On quantum rényi entropies: A new generalization and some properties,” *Journal of Mathematical Physics*, vol. 54, p. 122203, 2020/08/31 2013.
- [43] M. Kohmoto, “Entropy function for multifractals,” *Phys. Rev. A*, vol. 37, pp. 1345–1350, Feb 1988.
- [44] M. Janssen, “Statistics and scaling in disordered mesoscopic electron systems,” *Physics Reports*, vol. 295, no. 1, pp. 1 – 91, 1998.
- [45] A. De Luca, B. L. Altshuler, V. E. Kravtsov, and A. Scardicchio, “Anderson localization on the bethe lattice: Nonergodicity of extended states,” *Phys. Rev. Lett.*, vol. 113, p. 046806, Jul 2014.

Appendix A: Boundary conditions

In the main text, we derived Eq. (22), written here as

$$\cosh\left(2\frac{d\phi}{dm}\right) = \kappa(m), \quad \kappa(m) \equiv \frac{-\epsilon - f(m)}{\Gamma\sqrt{1-m^2}}. \quad (\text{A1})$$

At every m , this equation has two solutions:

$$\frac{d\phi}{dm} = \frac{1}{2} \log\left(\kappa(m) \pm \sqrt{\kappa(m)^2 - 1}\right). \quad (\text{A2})$$

Just as in one-dimensional tunneling problems, the boundary conditions determine which sign to use. Here, we show that the correct sign is $+$ near $m = -1$ and $-$ near $m = 1$. This then fixes the allowed values of ϵ , as discussed in the main text.

Starting from the Schrodinger equation, Eq. (19), first set $M = N - 2J$ with $J \ll O(N)$. To leading order in J/N , the equation simplifies to

$$\Psi(J+1) = -\frac{E + Nf(1)}{\Gamma\sqrt{N(J+1)}}\Psi(J) - \sqrt{\frac{J}{J+1}}\Psi(J-1). \quad (\text{A3})$$

The second term on the right-hand side will turn out to be subleading compared to the first, and so we omit it. Defining $\Phi(J) \equiv \log \Psi(J)$, we have

$$\Phi(J+1) = \Phi(J) + \frac{1}{2} \log \frac{N}{J+1} + \log \frac{-\epsilon - f(1)}{\Gamma}, \quad (\text{A4})$$

which can be easily solved:

$$\Phi(J) = \Phi(0) + J \log \frac{-\epsilon - f(1)}{\Gamma} + \frac{1}{2} \sum_{K=1}^J \log \frac{N}{K}. \quad (\text{A5})$$

This is an exact expression for the solution of the Schrodinger equation, which does not rely on taking any continuum limit.

Let us now compare Eq. (A5) to what we would find expanding the continuum Eq. (A2) in $1 - m$. Note that $\kappa(m) \rightarrow \infty$ as $m \rightarrow 1$ (at least for $\epsilon \neq f(1)$). Thus

$$\begin{aligned} \frac{d\phi}{dm} &\sim \pm \frac{1}{2} \log 2\kappa(m) \\ &\sim \pm \frac{1}{2} \log \frac{\sqrt{2}(-\epsilon - f(1))}{\Gamma} \mp \frac{1}{4} \log(1 - m). \end{aligned} \quad (\text{A6})$$

Integrating from $m = 1$ to $m = 1 - 2j$ gives

$$\phi(1-2j) = \phi(1) \mp j \log \frac{-\epsilon - f(1)}{\Gamma} \mp \frac{1}{2} \int_0^j dk \log \frac{1}{k}. \quad (\text{A7})$$

Comparing Eqs. (A5) and (A7) (noting that $\Phi(J) = N\phi(1 - 2j)$ by definition), we see that the lower sign is needed for the continuum result to agree with the exact expression.

A similar analysis holds near $m = -1$. Writing $M = -N + 2J$ and $\Phi(J) = N\phi(-1 + 2j)$, we find

$$\Phi(J) = \Phi(0) + J \log \frac{-\epsilon - f(-1)}{\Gamma} + \frac{1}{2} \sum_{K=1}^J \log \frac{N}{K}, \quad (\text{A8})$$

to be compared with

$$\phi(-1+2j) = \phi(-1) \pm j \log \frac{-\epsilon - f(-1)}{\Gamma} \pm \frac{1}{2} \int_0^j dk \log \frac{1}{k}. \quad (\text{A9})$$

The upper sign is needed for the two expressions to agree.

Thus a valid solution to the Schrodinger equation must indeed obey Eq. (A2) with the plus sign near $m = -1$ and the minus sign near $m = 1$.

Appendix B: Continuity of the surplus

Here we show that the surplus must approach 0 continuously as $\Gamma \rightarrow \Gamma_c$, for any symmetric model which meets the criteria given in the main text ($f(m)$ increasing monotonically with m and growing no faster than $O(m^2)$ near $m = 0$). We do so by proving that at Γ_c , $ds_1/dm \leq 0$ for all $m \geq 0$, with equality only at $m = 0$.

Since $s_1(m)$ varies continuously as Γ approaches Γ_c from below (it is only when the argmin of $U_-(m)$ jumps as Γ crosses Γ_c that there is a non-analyticity), this implies that for Γ infinitesimally less than Γ_c , the argmax of $s_1(m)$ cannot be at any non-infinitesimal m , i.e., μ_1 is continuous in Γ .

Without loss of generality, we can take $f(0) = 0$. At Γ_c , which is the field strength at which $U_-(0) = \epsilon_{GS}$, we thus have $\epsilon_{GS} = -\Gamma_c$. Then

$$\kappa(m) = \frac{\Gamma_c - f(m)}{\Gamma_c \sqrt{1 - m^2}}. \quad (\text{B1})$$

We thus write ds_1/dm as

$$\begin{aligned} \frac{ds_1}{dm} &= \frac{1}{4} \log \frac{1-m}{1+m} + \frac{1}{2} \log \left(\kappa(m) + \sqrt{\kappa(m)^2 - 1} \right) \\ &= \frac{1}{2} \log \frac{1}{1+m} + \frac{1}{2} \log \left(1 - \frac{f(m)}{\Gamma_c} + \sqrt{m^2 - 2\frac{f(m)}{\Gamma_c} + \frac{f(m)^2}{\Gamma_c^2}} \right). \end{aligned} \quad (\text{B2})$$

Since the minimum of $U_-(m)$ is not at $m = 1$, we know that

$$U_-(1) = -f(1) > \epsilon_{GS} = -\Gamma_c, \quad (\text{B3})$$

and since $f(m)$ is monotonic in m , it follows that for all $m \in [0, 1]$,

$$0 \leq f(m) < \Gamma_c. \quad (\text{B4})$$

We thus have the following chain of inequalities:

$$\begin{aligned} -2\frac{f(m)}{\Gamma_c} + \frac{f(m)^2}{\Gamma_c^2} &\leq 0 \\ \Rightarrow -2\frac{f(m)}{\Gamma_c} + \frac{f(m)^2}{\Gamma_c^2} &\leq m^2 \left(-2\frac{f(m)}{\Gamma_c} + \frac{f(m)^2}{\Gamma_c^2} \right) \\ \Rightarrow m^2 - 2\frac{f(m)}{\Gamma_c} + \frac{f(m)^2}{\Gamma_c^2} &\leq m^2 \left(1 - \frac{f(m)}{\Gamma_c} \right)^2 \\ \Rightarrow 1 - \frac{f(m)}{\Gamma_c} + \sqrt{m^2 - 2\frac{f(m)}{\Gamma_c} + \frac{f(m)^2}{\Gamma_c^2}} &\leq (1+m) \left(1 - \frac{f(m)}{\Gamma_c} \right). \end{aligned} \quad (\text{B5})$$

Inserting into Eq. (B2), we have simply

$$\frac{ds_1}{dm} \leq \frac{1}{2} \log \left(1 - \frac{f(m)}{\Gamma_c} \right). \quad (\text{B6})$$

Since $f(m)$ is monotonic and $f(0) = 0$, this establishes what we claimed: $ds_1/dm \leq 0$ with equality only at $m = 0$.

In fact, $s_1(m)$ has nice properties which allow us to determine the surplus quite simply. Starting from the upper line of Eq. (B2) and setting $ds_1/dm = 0$, we have

$$\kappa(m) + \sqrt{\kappa(m)^2 - 1} = \sqrt{\frac{1+m}{1-m}}. \quad (\text{B7})$$

Using the explicit expression for $\kappa(m)$ (note that here we are considering arbitrary Γ), this becomes

$$-\epsilon - f(m) + \sqrt{(\epsilon + f(m))^2 - \Gamma^2(1 - m^2)} = \Gamma(1 + m), \quad (\text{B8})$$

which simplifies considerably to (see also Ref. [15])

$$f(m) = -\epsilon - \Gamma. \quad (\text{B9})$$

The surplus is given merely by the solution to Eq. (B9).

This result holds for all Γ , and thus is quite useful in of itself. Furthermore, it gives an immediate alternate proof that the surplus is continuous at Γ_c (albeit one that does not generalize to other values of β): since ϵ approaches

$-\Gamma_c$ continuously as $\Gamma \rightarrow \Gamma_c$, the solution of Eq. (B9) for any monotonic $f(m)$ must approach 0 continuously.